

## Upper critical field, anisotropy, and superconducting properties of $\text{Ba}_{1-x}\text{K}_x\text{Fe}_2\text{As}_2$ single crystals

Zhao-Sheng Wang, Hui-Qian Luo, Cong Ren, and Hai-Hu Wen\*

National Laboratory for Superconductivity, Institute of Physics and Beijing National Laboratory for Condensed Matter Physics, Chinese Academy of Sciences, P.O. Box 603, Beijing 100190, People's Republic of China

(Received 20 August 2008; published 2 October 2008)

The temperature-dependent resistivity of  $\text{Ba}_{1-x}\text{K}_x\text{Fe}_2\text{As}_2$  ( $x=0.23, 0.25, 0.28,$  and  $0.4$ ) single crystals and the angle-dependent resistivity of superconducting  $\text{Ba}_{0.6}\text{K}_{0.4}\text{Fe}_2\text{As}_2$  single crystals were measured in magnetic fields up to 9 T. The data measured on samples with different doping levels revealed very high upper critical fields, which increase with the transition temperature, and a very low superconducting anisotropy ratio  $\Gamma = H_{c2}^{ab}/H_{c2}^c \approx 2$ . By scaling the resistivity within the framework of the anisotropic Ginzburg-Landau theory, the angle-dependent resistivity of the  $\text{Ba}_{0.6}\text{K}_{0.4}\text{Fe}_2\text{As}_2$  single crystal measured with different magnetic fields at a certain temperature collapsed onto one curve. As the only scaling parameter, the anisotropy  $\Gamma$  was alternatively determined for each temperature and was found to be between two and three.

DOI: 10.1103/PhysRevB.78.140501

PACS number(s): 74.25.Fy, 74.25.Op, 74.70.-b

Since the discovery of superconductivity at 26 K in the FeAs-based superconductor  $\text{LaFeAsO}_{1-x}\text{F}_x$ ,<sup>1</sup> great interest has been stimulated in the community of condensed-matter physics and material sciences. Under intensive study, the superconducting transition temperature ( $T_c$ ) was quickly promoted to 55 K by replacing La with Sm (Ref. 2) making the iron-based superconductors to be noncopper-based materials with  $T_c$  exceeding 50 K. At the same time, hole-doped superconductors were also synthesized successfully in  $\text{La}_{1-x}\text{Sr}_x\text{FeAsO}$  (Ref. 3) and  $\text{Ba}_{1-x}\text{K}_x\text{Fe}_2\text{As}_2$  (Ref. 4) systems. Beside the high critical temperature, the upper critical field was found to be very high in the iron-based superconductors.<sup>5-9</sup> Many theoretical models have been proposed to give explanations for the mechanism of superconductivity, such as nonphonon pairing mechanisms,<sup>10</sup> multi-band superconductivity,<sup>11</sup> etc. Meanwhile, many experiments have revealed evidence for an unconventional pairing mechanism in the single layer structure iron-based superconductors, such as point-contact tunneling spectroscopy,<sup>12</sup> NMR,<sup>13,14</sup> specific heat,<sup>15</sup> lower critical field,<sup>16,17</sup> etc. However, most of these measurements were carried out on polycrystalline samples because of the lack of sizable single crystals in the system with a single layer structure.

Fortunately, the  $\text{Ba}_{1-x}\text{K}_x\text{Fe}_2\text{As}_2$  single crystals can be grown by metal or by the self-flux method. With this success, more accurate measurements have become possible in this iron-based superconducting system. As one of the basic parameters, the superconducting anisotropy  $\Gamma = H_{c2}^{ab}/H_{c2}^c$  is crucial for both understanding the superconducting mechanism and the potential applications, where  $H_{c2}^{ab}$  and  $H_{c2}^c$  are the upper critical fields when the magnetic field is applied within the  $ab$  plane and  $c$  axis, respectively. With a layered structure in the FeAs-based superconductors, such as cuprates, strong anisotropy of superconductivity might be expected.<sup>18</sup> An estimation of  $\Gamma \geq 30$  was made on  $(\text{Nd}, \text{Sm})\text{FeAsO}_{0.82}\text{F}_{0.18}$  polycrystals from the  $c$ -axis infrared plasma frequency.<sup>17</sup> However, an anisotropy of about 4–6 for the upper critical field was found in  $\text{NdFeAsO}_{0.82}\text{F}_{0.18}$  single crystals<sup>7</sup> based on the transport measurements. Therefore, it is very necessary to determine the upper critical fields and the superconductivity anisotropy of the  $\text{Ba}_{1-x}\text{K}_x\text{Fe}_2\text{As}_2$  system espe-

cially for different doping levels. In this work, we present the temperature-dependent resistivity of  $\text{Ba}_{1-x}\text{K}_x\text{Fe}_2\text{As}_2$  ( $x=0.23, 0.25, 0.28,$  and  $0.4$ ) single crystals and the angle-dependent resistivity of  $\text{Ba}_{0.6}\text{K}_{0.4}\text{Fe}_2\text{As}_2$  single crystals. A very high upper critical field and a rather low superconductivity anisotropy were found. Both the upper critical field and the anisotropy  $\Gamma$  have been obtained for samples with different doping levels of potassium at different temperatures.

The single crystals of  $\text{Ba}_{1-x}\text{K}_x\text{Fe}_2\text{As}_2$  ( $0 < x \leq 0.4$ ) were grown by using FeAs as the self-flux at ambient pressures. During synthesis the FeAs content is several times higher than that of  $\text{Ba}_{1-x}\text{K}_x$ , and the actual composition of potassium is controlled by the growing temperature and the relative composition ratio between Ba and K. Details for the synthesis were described in Ref. 19. The composition of potassium given in this Rapid Communication is obtained from the energy dispersive x-ray (EDX) analysis spectrum. The typical lateral sizes of the crystals are about 2 to 3 mm, while thickness is about 0.1 mm. The good  $c$ -axis orientation of the crystals has been demonstrated by the x-ray diffraction (XRD) analysis which shows only the sharp  $(00\ell)$  peaks. The temperature-dependent ac susceptibility of the crystals were measured on an Oxford cryogenic system Maglab-EXA-12. During measurement, an alternating magnetic field ( $H=1$  Oe) perpendicular to the  $ab$  planes of the crystal at a frequency  $f=333$  Hz was applied. The susceptibility curve of a  $\text{Ba}_{0.6}\text{K}_{0.4}\text{Fe}_2\text{As}_2$  single crystal is shown in the inset of Fig. 1. The superconducting transition is very sharp with  $\Delta T_c < 0.5$  K ( $1\% \rho_n - 90\% \rho_n$ , where  $\rho_n$  is the normal-state resistivity) demonstrating the high quality and homogeneity of the single crystal.

The resistivity measurements were carried out on a physical property measurement system (PPMS) (Quantum Design) with magnetic fields up to 9 T. The electrical resistivity of  $\text{Ba}_{1-x}\text{K}_x\text{Fe}_2\text{As}_2$  ( $x=0.23, 0.25, 0.28,$  and  $0.4$ ) single crystals and the angle-dependent resistivity of  $\text{Ba}_{0.6}\text{K}_{0.4}\text{Fe}_2\text{As}_2$  single crystal were measured by the standard four-probe method. Figure 1 presents the in-plane resistivity  $\rho_{ab}$  of the  $\text{Ba}_{0.6}\text{K}_{0.4}\text{Fe}_2\text{As}_2$  single crystal in zero field up to 400 K. One can see that the  $\rho(T)$  data exhibit a continued curvature up to 400 K. In the angle-resolved resistivity measurement, the angle  $\theta$  was varied from  $0^\circ$  to  $180^\circ$ , where  $\theta=0^\circ$  corre-

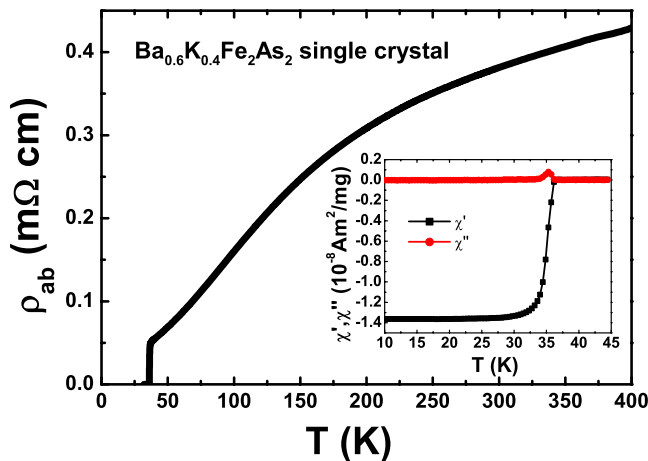


FIG. 1. (Color online) Temperature dependence of the in-plane electrical resistivity for a  $\text{Ba}_{0.6}\text{K}_{0.4}\text{Fe}_2\text{As}_2$  single crystal in zero field up to 400 K. One can see that the  $\rho_{ab}(T)$  curve exhibits a continued curvature up to 400 K. The inset shows the temperature-dependent ac susceptibility for the  $\text{Ba}_{0.6}\text{K}_{0.4}\text{Fe}_2\text{As}_2$  single crystal. Sharp superconducting transitions are obvious both in the resistive and in the ac susceptibility data.

sponded to the configuration of the  $H\parallel c$  axis and  $\theta=90^\circ$  to  $H\parallel ab$  plane, respectively. The current was applied in the  $ab$  plane and perpendicular to the magnetic field in all cases [as shown in the inset of Fig. 2(b)]. The sample with  $x=0.4$  exhibited a sharp resistive superconducting transition at  $T_c \approx 36.5$  K (90% of the normal-state resistivity) with  $\Delta T_c < 0.5$  K. The residual resistivity is about  $\rho(38\text{ K}) = 0.05$  m $\Omega$  cm and the residual resistivity ratio is found to be  $\text{RRR} = \rho(300\text{ K})/\rho(38\text{ K}) = 7.4$ .

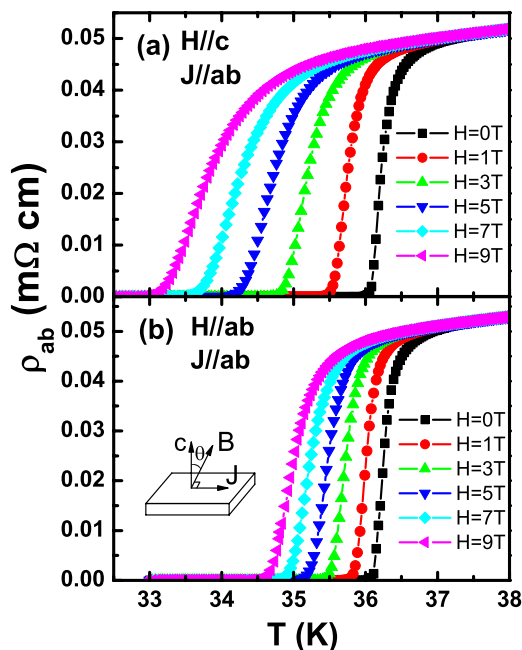


FIG. 2. (Color online) Temperature dependence of the in-plane electrical resistivity for the  $\text{Ba}_{0.6}\text{K}_{0.4}\text{Fe}_2\text{As}_2$  single crystal at fields  $\mu_0 H = 0, 1, 3, 5, 7, 9$  T with (a)  $H\parallel c$  and (b)  $H\parallel ab$ , respectively. The inset of (b) illustrates the definition of angle  $\theta$ .

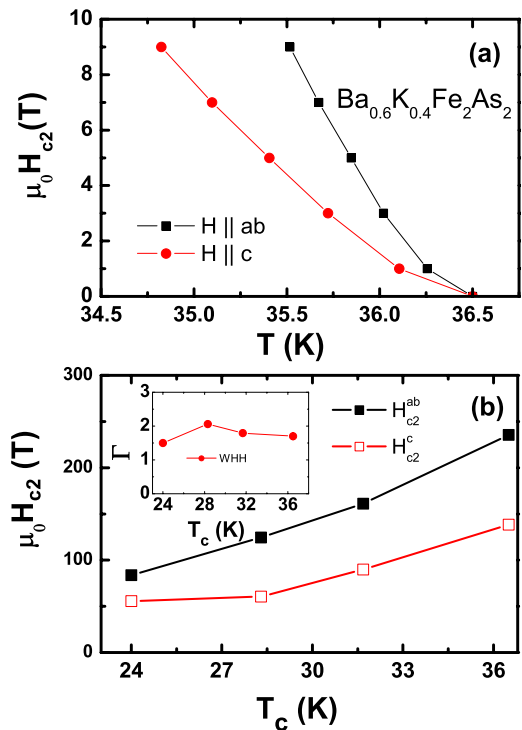


FIG. 3. (Color online) (a) The upper critical field of  $\text{Ba}_{0.6}\text{K}_{0.4}\text{Fe}_2\text{As}_2$  single crystal for  $H\parallel c$  and  $H\parallel ab$ , respectively. (b) The upper critical field versus  $T_c$  of  $\text{Ba}_{1-x}\text{K}_x\text{Fe}_2\text{As}_2$  crystals ( $x=0.23, 0.25, 0.28$ , and  $0.4$ ) and single crystals with  $T_c=24, 28.3, 31.7$ , and  $36.5$  K. The inset of (b) presents the anisotropy ratio of  $H_{c2}(0)$  along  $c$  axis and  $ab$  planes for the four samples. The lines are guides for the eyes.

Many experiments had revealed high upper critical fields in the  $\text{LnFeAsO}_{1-x}\text{F}_x$  (the estimated  $H_{c2}^{ab}$  is beyond 50 T for  $\text{Ln}=\text{La}$  and beyond 100 T for  $\text{Ln}=\text{Sm}, \text{Pr}$ , and  $\text{Nd}$ ) system.<sup>5-7</sup> In the  $\text{Ba}_{1-x}\text{K}_x\text{Fe}_2\text{As}_2$  system, the value of the upper critical field seems also very high.<sup>8,9</sup> Figures 2(a) and 2(b) show the temperature-dependent resistivity  $\rho(T)$  curves of the  $\text{Ba}_{0.6}\text{K}_{0.4}\text{Fe}_2\text{As}_2$  single crystal at magnetic fields up to 9 T along the  $c$  axis and  $ab$  planes, respectively. It is found that the superconducting transitions are broadened slightly, which indicates that the upper critical field should be very high. One can also see that the resistive transition curves shift parallel down to lower temperatures upon using a magnetic field; this may suggest a field-induced pair breaking effect in the present system. This is very different from the case in the cuprate superconductors where the  $\rho(T)$  broadens by exhibiting a fan structure with the onset transition part barely changed by the magnetic field. From the transition curves in Figs. 2(a) and 2(b), we already have an idea that the anisotropy ratio is quite small. In Fig. 3(a) we present the  $H_{c2}-T$  curves for the  $\text{Ba}_{0.6}\text{K}_{0.4}\text{Fe}_2\text{As}_2$  single crystal for both  $H\parallel c$  and  $H\parallel ab$ , respectively. The  $H_{c2}(T)$  is determined at the point where  $\rho=90\%\rho_n$ . The curves of  $H_{c2}(T)$  are very steep with average slopes  $-dH_{c2}^{ab}/dT|_{T_c} = 9.35$  T/K for  $H\parallel ab$  and  $-dH_{c2}^c/dT|_{T_c} = 5.49$  T/K for  $H\parallel c$ . According to the Werthamer-Helfand-Hohenberg (WHH) formula<sup>20</sup>  $H_{c2} = -0.69(dH_{c2}/dT)|_{T_c} T_c$  and taking  $T_c = 36.5$  K, the values of upper critical fields are  $H_{c2}^{ab}(0) = 235$  T and  $H_{c2}^c(0)$

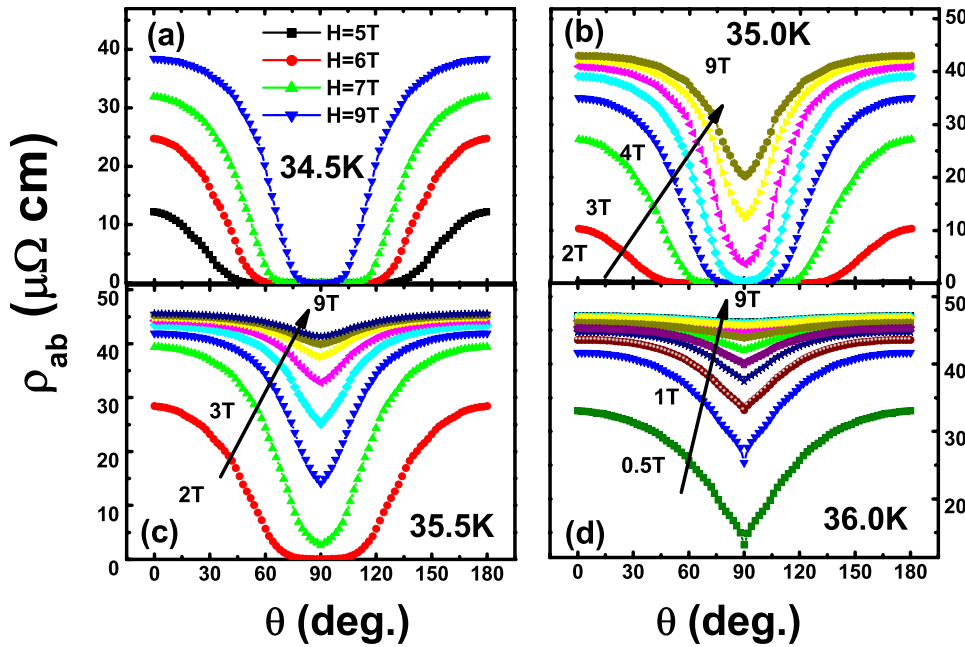


FIG. 4. (Color online) Angular dependence of resistivity at (a) 34.5 K in  $\mu_0 H = 5, 6, 7, 9$  T, (b) 35 K in  $\mu_0 H = 2, 3, 4, 5, 6, 7, 8, 9$  T, (c) 35.5 K in  $\mu_0 H = 2, 3, 4, 5, 6, 7, 8, 9$  T, and (d) 36 K in  $\mu_0 H = 0.5, 1, 1.5, 2, 2.5, 3, 4, 5, 6, 7, 8, 9$  T for the  $\text{Ba}_{0.6}\text{K}_{0.4}\text{Fe}_2\text{As}_2$  single crystal.

$= 138$  T. Although these high values of upper critical fields may be subject to a modification when the direct measurements are done in the high-field experiments, we believe that the FeAs-based superconductors are really robust against the magnetic field. For example, taking the zero-temperature values we obtained using the WHH formula, we have  $\mu_0 H_{c2}^{ab}(0)/k_B T_c = 235/36.5$  T/K = 6.43 T/K. This ratio is much beyond the Pauli limit  $\mu_0 H_{c2}(0)/k_B T_c = 1.84$  T/K for a singlet pairing when the spin-orbital coupling is weak.<sup>21</sup> This may manifest an unconventional mechanism of superconductivity in this material. The values of  $H_{c2}(0)$  for the other three samples with different doping levels of potassium and thus transition temperatures were also determined in the same way. The results are shown in Fig. 3(b). It is found that the  $H_{c2}(0)$  decreases quickly with the decrease in  $T_c$ . We note that a recent result reported that the WHH approximation may not be simply applied in these materials<sup>22</sup> and even  $H_{c2}(0)$  may be affected by the multiband property. However, our results clearly indicate that the upper critical fields in the present system are really very high without any doubt. The large value of the ratio  $\mu_0 H_{c2}^{ab}(0)/k_B T_c$  was also found in our previous measurements on  $\text{NdFeAsO}_{0.82}\text{F}_{0.18}$  single crystals.<sup>7</sup> As far as we know, the large value of the ratio  $\mu_0 H_{c2}(0)/k_B T_c$  obtained in FeAs-based superconductors has been rarely reported in other superconductors.

In an anisotropic type-II superconductor, the magnetic field destroys superconductivity at the upper critical fields  $H_{c2}^{ab}$  and  $H_{c2}^c$  for applied fields  $H \parallel ab$  and  $H \parallel c$ , respectively. The effective upper critical field varies between the two orientations depending on the superconducting anisotropy ratio  $\Gamma = H_{c2}^{ab}/H_{c2}^c$ . In the inset of Fig. 3(b), we show the doping dependence of the anisotropy ratio  $H_{c2}^{ab}(0)/H_{c2}^c(0)$  for the samples with different doping levels. One can see that the anisotropy for different samples all locate around two. This result is surprising to us since the band-structure calculations by Singh<sup>23</sup> clearly show that the Fermi-surface sheets and dimensionality strongly depend on the doping level. For the

$\text{Ba}_{0.6}\text{K}_{0.4}\text{Fe}_2\text{As}_2$  single crystal it is found that  $\Gamma \approx 1.70 \sim 1.86$  at zero temperature, and  $\Gamma$  is below 2.1 for all other samples. This value is quite close to that derived on similar samples also from the shift of the resistive transitions under magnetic fields.<sup>24</sup> The values of anisotropy are rather small in comparison with all cuprate superconductors and slightly lower than that of F-doped  $\text{NdFeAsO}$  with  $\Gamma = 4 - 6$ .<sup>7,25</sup>

The anisotropy ratio determined above may be subject to a modification because of the uncertainties in determining the upper critical field value by taking different criterions of resistivity and by using different formulas. One major concern was that the zero-temperature value  $H_{c2}(0)$  was determined by using the experimental data near  $T_c$ . This concern can be removed by the measurements of angular-dependent resistivity. According to the anisotropic Ginzburg-Landau theory, the resistivity in the mixed state depends on the effective field  $H/H_{c2}^{\text{GL}}(\theta)$ . In this case the resistivity measured at different magnetic fields but at a fixed temperature should be scalable with the variable  $H/H_{c2}^{\text{GL}}(\theta)$ . The effective upper critical field  $H_{c2}^{\text{GL}}(\theta)$  at an angle  $\theta$  is given by

$$H_{c2}^{\text{GL}}(\theta) = H_{c2}^c / \sqrt{\cos^2(\theta) + \Gamma^{-2} \sin^2(\theta)}. \quad (1)$$

Thus using the scaling variable  $\tilde{H} = H \sqrt{\cos^2(\theta) + \Gamma^{-2} \sin^2(\theta)}$ , the resistivity should collapse onto one curve in different magnetic fields at a certain temperature<sup>26</sup> when an appropriate  $\Gamma$  value is chosen. Figure 4 presents four sets of data of angular dependence of resistivity at 34.5, 35, 35.5, and 36 K for the  $\text{Ba}_{0.6}\text{K}_{0.4}\text{Fe}_2\text{As}_2$  single crystal. At each temperature, a cup-shaped feature centered around  $\theta = 90^\circ$  is observed. As shown in Fig. 5, the curves measured at different magnetic fields, but at a fixed temperature, are scaled nicely by adjusting  $\Gamma$ . The values of  $\Gamma$  were thus obtained for temperatures 34.5, 35, 35.5, 36, and 36.5 K. Because only one fitting parameter  $\Gamma$  is employed in the scaling for each temperature, the value of  $\Gamma$  is more reliable compared with the one determined from the ratio of

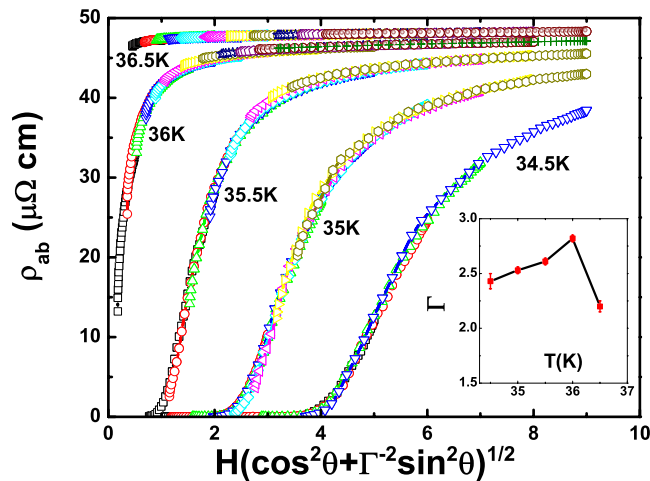


FIG. 5. (Color online) Scaling of the resistivity versus  $\tilde{H} = H\sqrt{\cos^2(\theta) + \Gamma^{-2}\sin^2(\theta)}$  at 34, 34.5, 35, 35.5, 36, 36.5, and 37 K in different magnetic fields. Each curve is scaled nicely by adjusting  $\Gamma$ . The inset presents the temperature-dependent  $\Gamma(T)$  for the  $\text{Ba}_{0.6}\text{K}_{0.4}\text{Fe}_2\text{As}_2$  single crystal. The line is a guide for the eyes.

$H_{c2}^{ab}$  and  $H_{c2}^c$  as used above. But both methods yield similar values of  $\Gamma$ , which implies the validity of the values determined in this work. It is found that the anisotropy increases from 2.43 for 34.5 K to 2.82 for 36 K and then decreases slightly for 36.5 K as plotted in the inset of Fig. 5. Actually the anisotropy was also measured to the much higher field and lower temperature region<sup>8,9</sup> in the same system, was found to decrease with temperature, and finally reached a value of about 1–1.5 in the low  $T$  limit. This kind of tem-

perature dependence of  $\Gamma(T)$  is not expected for a single band anisotropic superconductor and needs a further check in other measurements. It may be attributed to the effect of the two-gap scenario.<sup>27–30</sup> In addition, it should be noted that the good scaling behavior suggests a field-independent anisotropy in the temperature and field range we investigated. The small anisotropy can be qualitatively understood based on the recent band-structure calculations<sup>23</sup> in which it is shown that the Fermi-surface sheets are not two-dimensional (2D) cylinderlike but rather exhibit a complicated three-dimensional (3D) feature with a quite strong dispersion along the  $c$  axis. Our results here—very high upper critical fields and very low anisotropy—should be stimulating in fulfilling a quantitative calculation on the electronic structure of the doped samples and ultimately providing an understanding to the underlying mechanism of superconductivity.

In conclusion, we have investigated the temperature-dependent resistivity for  $\text{Ba}_{1-x}\text{K}_x\text{Fe}_2\text{As}_2$  ( $0 < x \leq 0.4$ ) single crystals in magnetic fields up to 9 T. It is found that the system poses a very high upper critical field and a very low superconducting anisotropy ratio which is around two for all the samples. In an alternative way, we also determined the anisotropy ratio by investigating the angle-dependent resistivity in the  $\text{Ba}_{0.6}\text{K}_{0.4}\text{Fe}_2\text{As}_2$  single crystals. Both methods yield the similar values of the anisotropy ratio  $\Gamma$ . Our results strongly suggest that the anisotropic Ginzburg-Landau theory can be used to describe the data in the mixed state very well.

This work is supported by the Natural Science Foundation of China, the Ministry of Science and Technology of China (973 Projects No 2006CB60100, No. 2006CB921107, and No. 2006CB921802), and the Chinese Academy of Sciences (Project ITSNEM).

\*hhwen@aphy.iphy.ac.cn

- <sup>1</sup>Y. Kamihara *et al.*, J. Am. Chem. Soc. **130**, 3296 (2008).
- <sup>2</sup>Z. A. Ren *et al.*, Chin. Phys. Lett. **25**, 2215 (2008).
- <sup>3</sup>H. H. Wen *et al.*, EPL **82**, 17009 (2008).
- <sup>4</sup>M. Rotter *et al.*, Phys. Rev. Lett. **101**, 107006 (2008).
- <sup>5</sup>X. Y. Zhu *et al.*, Supercond. Sci. Technol. **21**, 105001 (2008).
- <sup>6</sup>F. Hunte *et al.*, Nature (London) **453**, 903 (2008).
- <sup>7</sup>Y. Jia *et al.*, Appl. Phys. Lett. **93**, 032503 (2008).
- <sup>8</sup>M. Altarawneh *et al.*, arXiv:0807.4488 (unpublished).
- <sup>9</sup>H. Q. Yuan *et al.*, arXiv:0807.3137 (unpublished).
- <sup>10</sup>L. Boeri *et al.*, Phys. Rev. Lett. **101**, 026403 (2008).
- <sup>11</sup>L. Benfatto *et al.*, arXiv:0807.4408 (unpublished).
- <sup>12</sup>L. Shan *et al.*, EPL **83**, 57004 (2008).
- <sup>13</sup>H. J. Grafe *et al.*, Phys. Rev. Lett. **101**, 047003 (2008).
- <sup>14</sup>K. Matano *et al.*, EPL **83**, 57001 (2008).
- <sup>15</sup>G. Mu *et al.*, Chin. Phys. Lett. **25**, 2221 (2008).

- <sup>16</sup>C. Ren *et al.*, arXiv:0804.1726 (unpublished).
- <sup>17</sup>A. Dubroka *et al.*, Phys. Rev. Lett. **101**, 097011 (2008).
- <sup>18</sup>D. J. Singh and M. H. Du, Phys. Rev. Lett. **100**, 237003 (2008).
- <sup>19</sup>H. Q. Luo *et al.*, arXiv:0807.0759 (unpublished).
- <sup>20</sup>N. R. Werthamer *et al.*, Phys. Rev. **147**, 295 (1966).
- <sup>21</sup>A. M. Clogston, Phys. Rev. Lett. **9**, 266 (1962).
- <sup>22</sup>G. Fuchs *et al.*, arXiv:0806.0781 (unpublished).
- <sup>23</sup>D. J. Singh, arXiv:0807.2643 (unpublished).
- <sup>24</sup>N. Ni *et al.*, Phys. Rev. B **78**, 014507 (2008).
- <sup>25</sup>Y. Jia *et al.*, Supercond. Sci. Technol. **21**, 105018 (2008).
- <sup>26</sup>G. Blatter *et al.*, Phys. Rev. Lett. **68**, 875 (1992).
- <sup>27</sup>Q. Han *et al.*, EPL **82**, 37007 (2008).
- <sup>28</sup>V. Cvetkovic and Z. Tesanovic, arXiv:0804.4678 (unpublished).
- <sup>29</sup>H. Ding *et al.*, EPL **83**, 47001 (2008).
- <sup>30</sup>C. Ren *et al.*, arXiv:0808.0805 (unpublished).